Unloading method in coordinated harvesting

Xiaoxiong Wang[1,2], Zhihong Man[3*], Zhuo Wang[1], Xiaoping Bai[1], Jian Wang[1,2], Zhikang Ge[1,2]

(1. *Shenyang Institute of Automation, Chinese Academy of Sciences, Shenyang 110016, China*;
2. *School of Computer Science and Technology, University of Chinese Academy of Sciences, Beijing 100049, China*;
3. *School of Software and Electrical Engineering, Swinburne University of Technology, Melbourne, VIC3122, Australia*)

Abstract: In this study, a novel unloading method was developed for the operation of the unloading spout during the loading process in a master-slave automatic harvesting system. It demonstrated that uniform and full loading in the grain tank can be achieved by uninterrupted unloading with the motion of the unloading spout. First, the overflow algorithm is proposed to divide the loading process into multiple loading rounds. In each round, a specific loading area and target loading height are assigned to achieve better uniformity. Subsequently, complete coverage path planning and transfer path planning algorithms are developed to guide the motion of the unloading spout during different loading rounds. With the motion of the unloading spout, loading can be carried out accurately to maximize the capacity utilization of the grain tank, which can reduce the round-trip frequency of the transport vehicle and improve the energy and time efficiency of the harvesting operation. Simulation results are provided to validate the excellent performance of the presented unloading method.

Keywords: coordinated harvesting, loading uniformity, overflow algorithm, path planning
DOI: 10.25165/j.ijabe.20251802.8863

Citation: Wang X X, Man Z H, Wang Z, Bai X P, Wang J, Ge Z K. Unloading method in coordinated harvesting. Int J Agric & Biol Eng, 2025; 18(2): 45–54.

1 Introduction

With the impact of climate change and the pressure of population growth, grain production is facing increasing challenges[1]. Given the brief optimal harvest window for grains, it is necessary to harvest a substantial amount of grain within a limited timeframe to improve quality and yield[2-4]. Thus, enhancing the efficiency of grain harvesting to ensure timely harvesting is of great significance.

As efficient harvesting equipment, combine harvesters are widely employed for harvest operations. Since the capacity of the harvester's grain hopper is limited, regular unloading during harvesting is necessary. The process of unloading involves transferring grains from the grain hopper onboard the combine harvester to a tractor-towed grain tank. To expedite this process, Kurita et al. developed an automated unloading system that can identify the carriage and locate the unloading spout to the center of the grain tank to complete the unloading[5-7]. Several algorithms have been developed to optimize unloading operations, aiming to reduce the overall unloading time[8]. Nevertheless, unloading itself is time-consuming[9,10]. In response to this challenge, cooperative unloading has emerged as a desirable operation. During cooperative unloading, the harvester continues harvesting while simultaneously unloading grains to a transporter alongside it, thereby reducing unproductive time for the harvester[11]. Several researchers have developed cooperative control methods ensuring that the grain tank is always positioned under the unloading spout to collect grains[12]. Delchev et al.[13] demonstrated that on-the-go unloading can result in up to a 30% reduction in downtime per unit area during harvesting.

Due to the limited flowability of grains, they tend to form a pile rather than a flat surface when unloaded at a fixed location. Therefore, the position of the unloading spout should neither be rigidly fixed at the center of the grain tank, nor altered arbitrarily. Instead, the position should be adjusted based on the loading state of the grain tank to achieve an optimal loading effect. The motion of the unloading spout should attempt to achieve the following objectives: 1) maximize the filling of the grain tank; 2) maintain a uniform loading state during unloading; and 3) complete the unloading process as quickly as possible.

Liu et al.[14] divided the grain tank into several subregions and determined the movement strategy of unloading spouts by detecting the loading status of each subregion. Wang et al.[15] divided the grain tank based on the angle of repose of the grain and subsequently moved the unloading spout to fill each area sequentially. The partitioned loading method that they applied indeed increased the loading quantity in the grain tank, which improved productivity in grain transfer logistics. However, this process results in poor uniformity during loading. While some areas become full, other areas remain empty. The significant height difference between adjacent areas risked grain slippage to lower loading areas during bumps, leading to a lower-than-expected loading quantity. To address this issue, Liu et al.[16] performed multiple rounds of loading on each subregion to achieve the desired loading level. In these methods, the unloading spout remains centered in the lateral location, with adjustments made only in the longitudinal direction, limiting the unloading range inside the grain tank. Additionally, the conservative loading strategy adopted to prevent spillage, stemming from low detection accuracy of the loading state, inadvertently reduced the loading quantity.

In fact, loading the area on both sides of the grain tank by the

Received date: 2024-02-16 **Accepted date:** 2025-02-24
Biographies: **Xiaoxiong Wang**, PhD candidate, research interest: intelligent harvesting machinery, Email: wangxiaoxiong@sia.cn; **Zhuo Wang**, Professor, interest: AI for science, Email: zwang@sia.cn; **Xiaoping Bai**, Professor, research interest: agricultural machinery and equipment, Email: baixiaopin@sia.cn; **Jian Wang**, PhD candidate, research interest: image processing, Email: wangjian6@sia.cn; **Zhikang Ge**, PhD, research interest: sliding mode control method, Email: gezhikang@sia.cn.
***Corresponding author: Zhihong Man**, Professor, research interest: pattern recognition and intelligent control. Swinburne University of Technology, John Street, Hawthorn, Victoria 3122, Australia; Tel: +61-3-92145000; Email: zman@swin.edu.au.

lateral relative movement of the unloading spout is also essential for maintaining the uniformity of loading in the grain tank of transport vehicles. This factor is taken into consideration in the dynamic uniform loading method[17]. Benefiting from the application of high-precision sensors, the loading state can be detected more accurately, allowing for the subdivision of the workspace into finer grid cells both laterally and longitudinally. Recent advancements in cooperative control technology have achieved precise position control of the unloading spout, which enables accurate unloading at the designated position[12,18-20]. Instead of loading continuously until the current cell becomes full, the dynamic uniform loading method employs a staged loading approach. In each stage, the cell with the least amount of grain is selected and loaded with a constant quantity of grain, progressively filling the grain tank until full. However, positions continuous in the loading sequence may not correspond to adjacent locations. The unloading process experiences interruptions when the unloading spout travels between nonadjacent unloading positions. Frequent interruptions in the unloading process extend the overall loading time. While the dynamic uniform loading method successfully accomplished objectives 1 and 2, it was insufficient for achieving objective 3, which involves quick loading. The increased unloading time extends the unnecessary collaborative movement distance of the transport vehicle, leading to additional fuel consumption. In a subsequent study, Wang et al. designed a continuous path to guide the unloading spout for uninterrupted unloading in a grain tank[21]. However, the path is suitable only for scenarios involving loading from an empty grain tank or a uniformly loaded grain tank, posing challenges in adapting to different initial loading states. A loading path that can guide the unloading spout to achieve uniform full loading in the grain tank from an arbitrary loading state without any interruption is urgently needed.

The unloading spout needs to access all the subregions in the grain tank to achieve uniform full loading. Although many path planning methods have been developed[22,23], they are not suitable for determining the movement of the unloading spout. On the one hand, the access order of the unloading spout is related to the loading quantity on each subregion. Given an arbitrary initial loading state, sequentially loading each subregion in the order of loading quantity from lowest to highest yields the best loading uniformity. However, it is almost impossible for a continuous path to access the discretization region in this order. On the other hand, the loading of each region is not completed at once; instead, it is done layer by layer to improve the uniformity of the loading process. The loading increments in each subregion not only determine the current loading uniformity but also impact subsequent loading processes. Planning a path for the unloading spout that enables continuous unloading with appropriate increments to maximize uniformity during loading is challenging.

In this paper, we develop a novel path planning method to guide the movement of the unloading spout during loading. The loading path is constructed by the overflow algorithm, which simulates the water flow in valley submergence. While the unloading spout moves along the planned continuous path, the grains from the spout fill low-load areas, similar to how water fills low-lying areas. The study of the kinematic model shows that the planned path can be executed by the cooperative system. By performing continuous unloading along the path, the areas with low loading are gradually filled to improve the loading uniformity and ultimately achieve a uniform loading state.

The rest of this paper is organized as follows. In Section 2, the kinematic model of the harvesting system is studied first. Then the uniformity of loading is defined. The overflow planning method is subsequently developed to generate paths to guide the motion of the unloading spout in the grain tank. In Section 3, numerical simulations are carried out to illustrate the excellent performance of the loading path planning method proposed in this paper. Section 4 gives the main conclusions.

2 Materials and methods

2.1 Kinematics of the harvesting system

In this section, the kinematics of the harvesting system consisting of combine harvester and transport vehicle is studied to determine the workspace of the unloading spout. As shown in Figure 1, the grain tank on the transport vehicle is denoted by a rectangle with a size of $a \times b$. The unloading arm of length l is installed at point O of the harvester and can rotate around point O. The unloading spout is located at the free end of the unloading arm. The distance between point O and the front side of the grain tank is l_f, which is negative when point O is beyond the grain tank in the direction of travel. The distance between point O and the near side of the grain tank is d.

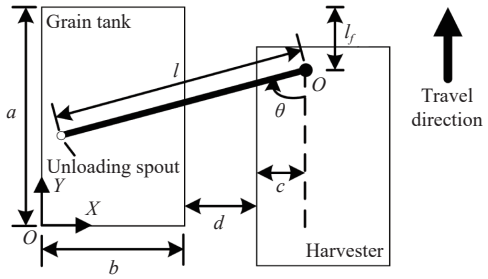

Figure 1 Kinematics model of harvesting system

Establishing a coordinate system XoY with the point in the lower left corner of the grain tank as the origin, the coordinates of the unloading spout (x,y) can be expressed as

$$\begin{cases} x = b + c + d - l\sin\theta \\ y = a - l_f - l\cos\theta \end{cases} \tag{1}$$

where, a, b, c, and l are the known positive constant parameters for an instantiated agricultural machinery; the horizontal distance $d \in (0,+\infty)$, the vertical relative distance $l_f \in [-\infty,+\infty]$, as well as the rotation angle $\theta \in [0,\pi/2]$ are the system state variables. Considering the value range of system variables d, l_f, and θ, and the value of constants a, b, c, and l in (1), the feasible region of the unloading spout can be expressed as

$$P = \{(x,y) | b + c + d - l \le x \le b + c + d, -\infty < y < +\infty\} \tag{2}$$

The two-dimensional space within the grain tank can be defined as

$$Q = \{(m,n) | 0 < m < b, 0 < n < a\} \tag{3}$$

In order to ensure the unloading spout can reach everywhere in the grain tank, the feasible region of the unloading spout must cover all the space of the grain tank in a two-dimensional plane. Thus, the inclusion relationship between Q and P in Equations (2) and (3) can be expressed as

$$Q \subseteq P \tag{4}$$

Combinning Equations (2) and (3) with (4):

$$\begin{cases} b + c + d - l \le 0 \\ b + c + d \ge 0 \end{cases} \tag{5}$$

Then we have

$$0 < d \le l - b - c \tag{6}$$

To make sure there are valid solutions d in (6), constant values b, c, and l must satisfy the condition as

$$l > b + c \tag{7}$$

Although the horizontal distance d is variable in the range of condition (6), it is expected to be set as a constant for dimension reduction and to simplify the calculation. On the one hand, maximizing the distance d between two vehicles can improve the safety of driving. On the other hand, when $d < l - b - c$, the available rotation angle range of the unloading arm is decreased, which leads to the decrement of resolution accuracy on the lateral position of the unloading spout. Based on the considerations above, the distance d is set as:

$$d = l - b - c \tag{8}$$

Then (1) can be expressed as

$$\begin{cases} x = l - l\sin\theta \\ y = a - l_f - l\cos\theta \end{cases} \tag{9}$$

whose solution can be expressed as

$$\begin{cases} \theta = atan2\left(l - x,\ \sqrt{l^2 - (l-x)^2}\right) \\ l_f = a - y - l\cos\theta \end{cases} \tag{10}$$

with

$$atan2(v,u) = \begin{cases} \arctan\left(\dfrac{v}{u}\right),\ u > 0 \\ \arctan\left(\dfrac{v}{u}\right) + \pi,\ u < 0, v \ge 0 \\ \arctan\left(\dfrac{v}{u}\right) - \pi,\ u < 0, v < 0 \\ \pi/2,\ u = 0, v > 0 \\ -\pi/2,\ u = 0, v < 0 \\ 0,\ u = 0, v = 0 \end{cases} \tag{11}$$

Thus, by maintaining a constant distance $d = l - b - c$ between the vehicles, the unloading spout can reach any target point within the grain tank $(x,y) \in Q$, through the combination of adjusting the longitudinal relative distance l_f and the rotation angle θ as (10).

Remark 1: Since the unloading spout can reach everywhere in the grain tank when the condition (7) is satisfied, the entire grain tank can be designated as the workspace for subsequent path planning of the unloading spout. This means that all positions within the grain tank can be loaded, allowing for precise control of the loading uniformity.

2.2 Loading uniformity

The loading state undergoes dynamic changes during the loading process. To compare the uniformity across different loading states, it is necessary to quantify the loading states. In this paper, a grid map is constructed by discretizing the underside of the grain tank into N grid cells with the same size and shape. These cells collectively form a two-dimensional representation of the grain tank. The virtual height of each 2D cell is defined by the average height of the grain surface within that cell. Assuming an equal density of grain piles, the quantity of grains within each cell can be expressed by the height of the grid cell. Consequently, the loading state of the grain tank is effectively characterized by the heights of these cells as

$$G = \{h_i, i = 1, 2, \ldots, N\} \tag{12}$$

where, h_i is the height of the ith grid cell. Then, the uniformity of the loading state can be described by the variance of height as

$$\sigma^2 = \frac{1}{N}\sum_{i=1}^{N}\left(h_i - \bar{h}\right)^2 \tag{13}$$

where, $\bar{h} = \dfrac{1}{N}\sum_{i=1}^{N} h_i$ is the average height of the grain surface in the whole grain tank. It should be noted that the smaller σ^2 is, the better the loading uniformity is.

For an initial loading state G_0, the uniformity after loading at the jth grid cell can be expressed as

$$\begin{aligned} \sigma_1^2 = &\frac{1}{N}\left\{\sum_{i=1, i\ne j}^{N}\left(h_i - \bar{\tilde{h}}\right)^2 + \left(h_j + \tilde{h} - \bar{\tilde{h}}\right)^2\right\} = \\ &\frac{1}{N}\sum_{i=1}^{N}\left(h_i - \bar{\tilde{h}}\right)^2 + \frac{1}{N}\left\{\tilde{h}^2 + 2\tilde{h}\left(h_j - \bar{\tilde{h}}\right)\right\} = \\ &\sigma_0^2 + \frac{\tilde{h}^2}{N} + \frac{2\tilde{h}}{N}\left(h_j - \bar{\tilde{h}}\right) \end{aligned} \tag{14}$$

where, h_j is the height of the j^{th} grid cell, $\tilde{h}$ is the height increment of the j^{th} grid cell, $\bar{\tilde{h}} = (N\bar{h} + \tilde{h})/N$ is the average height of the grain surface after loading, and σ_0^2 is the uniformity loading state G_0. It is observed that, given a loading increment $\tilde{h}$, the smaller the value of h_j is, the smaller the value of σ_1^2. This implies that loading should be carried out at the lower grid cell to ensure better loading uniformity.

2.3 Overflow planning method

It can be obtained from Equation (14) that loading should be initiated at the lowermost grid cell and progressively proceed to the higher cells. However, attempting to load cells in height order may lead to inefficiency due to the time lost in transferring between nonadjacent cells, given the disordered distribution of cell heights on the grid map.

In this section, a path planning method is proposed to visit only a few carefully selected contiguous cells in each loading round, ensuring continuous loading without interruptions caused by transfers. First, the overflow algorithm is developed to delineate a specific area within the workspace for effective path planning in each loading round. Then, two path planning algorithms are introduced: an improved Glasius bio-inspired neural network (GBNN)[24] algorithm for complete coverage path planning and a breadth-first search-based algorithm for point-to-point path planning. The choice of the algorithm for each loading round depends on the results of the overflow algorithm. By planning a path in each loading round to guide the motion of the unloading spout during continuous loading, a uniform full loading state for the grain tank is achieved. Here, a loading round is defined as an operation that delineates a specific area within the workspace and loads the area to the target height along the planned path.

2.3.1 Overflow algorithm

The overflow algorithm is developed based on the following process of valley submergence. For convenience, the cross section of the valleys is shown in Figure 2a, with three local minima at valleys 1, 2, and 3, in rounds. The water is poured continuously at the global lowest point in valley 1. Initially, the water is above the minimum point of valley 1 and gradually rises to the level of h_1, matching the adjacent lowest mountain peak, as shown in Figures 2a and 2b. As more water is poured, the water overflows

from the peak into valley 2, as shown in Figure 2c, to reach the level of h_2. Gradually, as shown in Figures 2d and 2f, all the locations in the three valleys are filled with water, resulting in a common uniform water surface. It is worth noting that during the whole process, the water always stays in the lowest area it can reach. By conceptualizing the initial loading state in the grain tank as a continuous valley and filling with grains as water floods the valley, not only the uniform full loading result but also the optimal uniformity during loading can be achieved.

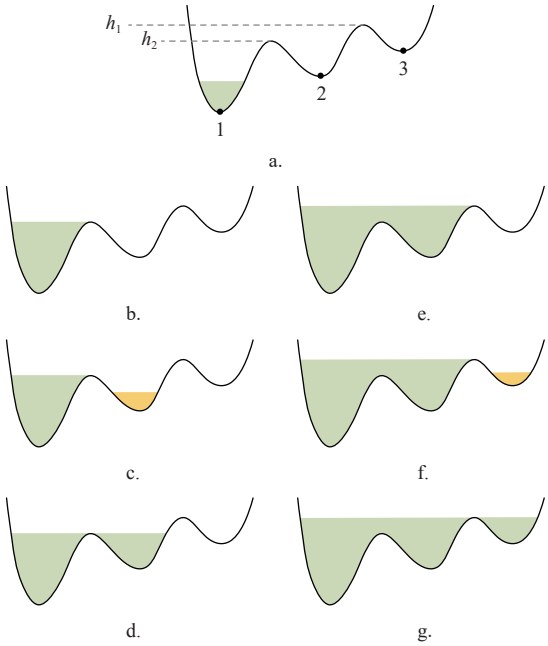

Figure 2 Diagram of the overflow algorithm

Although the grains are not a fluid and tend to form a heap rather than a flat surface during continuous pouring at a fixed position, the unloading spout can be strategically maneuvered to facilitate the "flow" of the grains into the adjacent lower areas. The continuity of water flow implies that loading can proceed continuously. Therefore, the principle of valley submergence as discussed above may be referenced to design the motion path of the unloading spout in the loading process. The unloading spout is initially located at the lowest area and progressively expands the range of motion to fill the valley with grains. Consecutively, the motion path for the unloading spout can be scheduled valley-by-valley in the same manner. Finally, the process of loading a full tank of grains with a relatively flat surface is completed.

To facilitate algorithm implementation in practice, the overflow loading process can be designed as follows. Initially, only the cell with the lowest height is assigned as the loading area. When loading on a cell, the loading quantity can be adjusted by the duration for which the unloading spout stays on. Since the loading increment cannot be infinitesimally small, $\Delta h_{\min}$ is used to represent the minimum height increment in a grid cell during a single loading round. After the initial cell is filled from the current height h_a to its lowest neighboring cell h_d, the range of the loading area should be expanded, similar to how water spreads to submerge the surrounding area as the level rises. Thus, the target height on the initial cell in the first loading round is set as the larger value between $h_a+\Delta h_{\min}$ and h_d. Then, the value of h_a is updated to the target height, and the loading area is reassigned.

Before each reassignment of the loading area, it is necessary to determine whether the loading area is expanded on the original basis or transferred to a new location. To do this, the cells adjacent to the last loading area are visited to identify the candidate cells with a height no greater than h_a. The cells adjacent to candidate cells are also added to the visit list. When visiting the cells adjacent to a candidate cell, the cells no higher than the candidate cell are also marked as candidate cells. After all the candidate cells have been identified, the lowest candidate cell is determined. If the lowest candidate cell is higher than $h_a-\Delta h_{\min}$, the loading area is expanded as shown in Figures 2a and 2b. Otherwise, loading should be transferred to another low area, similar to what occurs when water overflows, as shown in Figures 2b and 2c.

In the first case, the middle value of $h_a+\Delta h_{\min}$, $h_a+\Delta h_{\max}$, and h_d is taken as the target level for the next loading round, where the constant $\Delta h_{\max}$ is set to limit the maximum height increments in a grid cell during a single loading round. The loading area is expanded by merging adjacent cells whose height is no more than $\Delta h_{\min}$ lower than the target level. The cells adjacent to the merged cells are also taken into consideration. Then, the unloading spout is expected to move within the loading area to fill all the cells to the target level. The method of complete coverage path planning for the unloading spout in the loading area is introduced in Section 2.3.2.

In the latter case, the grains should overflow to the location of the lowest candidate cell in the subsequent loading process. The transfer path of the unloading spout to help the grains "flow" to the local lowest point is described in Section 2.3.3. Notably, all the identified candidate cells form the workspace of the transfer path planning. Then, the loading area is reassigned to the lowest candidate cell, and the target height is set as the initial stage on the initial cell.

After the loading area and target height are assigned for each loading round, the loading area is expected to reach the target height via the motion of the unloading spout. Such "valley filling" continues until the grain tank achieves uniform full loading. The above discussions are summarized by the following algorithm:

Algorithm 1: Overflow algorithm

input: current loading state, $h_{\min}$ and $h_{\max}$
output: parameters for movement path planning
Initialization;
Search the cell with the lowest height;
Build initial loading area;
Fill the loading area to target height;
Update the loading state and parameters h_a and h_d;
while the grain tank is not uniformly full
  search the candidate cells;
  if the lowest candidate cell is lower than $h_a-\Delta h_{\min}$
    output the parameters for the transfer path planning;
  else
    select the target height;
    assign the loading area;
    output the parameters for complete coverage path planning;
  end
  Update the loading state and parameters h_a and h_d;
end

Remark 2: The loading is divided into two different modes: accumulation and overflow. In the accumulation stage, loading is performed in layers within a gradually expanding area. Once the local area is filled in, the loading spout is transferred to another low-lying area to repeat the accumulation stage. These two modes, accumulation and overflow, are alternated to achieve uniform full loading. Throughout the loading process, the overflow algorithm

always attempts to guide the loading performed in as low an area as possible to obtain better loading uniformity.

Remark 3: Since the workspace of path planning for the former loading round is encompassed by that for the later round, the paths of all the adjacent rounds are connected when the endpoint of the former round serves as the start point of the later round. The overflow algorithm ensures that the designed loading process in the grain tank can be performed by the unloading spout with uninterrupted unloading along continuous motion paths.

2.3.2 Complete coverage path planning

In this section, the GBNN is improved to generate a complete coverage path for the unloading spout to meet the requirement of the overflow algorithm that all the cells in the loading area be loaded to the target level in specific loading rounds.

An example of the loading area, painted in gray and created from the overflow algorithm in a 10×10 grid map, is shown in Figure 3a. The corresponding state space of the neural network is shown in Figure 3b. Each cell in the grid map represents a neuron in the neural network (denoted by circles). For the 10×10 grid map, the corresponding neural network is a 10×10 topology in which all the neurons are connected to the other neurons within the receptive field. The receptive field of a neuron can be considered as a circle with a radius of R. Different from the original GBNN, lateral connections exist in only four directions instead of eight directions, aiming to avoid oblique paths, which is difficult to perform.

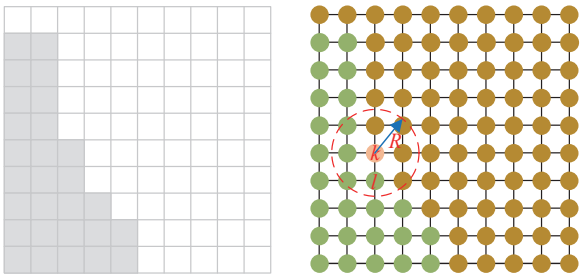

a. Grid map b. Neural network

Figure 3 Workspace representation

The connection weight w_{kl} between the kth neuron and any other l-th neuron can be defined as

$$w_{kl} = \begin{cases} e^{-\alpha|k-l|^2}, & 0 < |k-l| \le R \\ 0, & |k-l| > R \end{cases} \tag{15}$$

where, $|k-l|$ is the Euclidean distance between the kth and lth neurons, andα and R are all positive constants. The connection weight with a neuron outside of the receptive field is set to zero because the neurons are not connected. The neuron activity of the kth neuron at the t+1 time step, $x_k(t+1)$, is governed by the dynamic behavior as

$$x_k(t+1) = g\left(\sum_{l=1}^{N} w_{kl}[x_l(t)]^+ + I_k\right) \tag{16}$$

with the transfer function

$$g(x) = \begin{cases} -1, & x < 0 \\ \beta x, & 0 < x < 1 \\ 1, & x \ge 1 \end{cases} \tag{17}$$

where, N is the number of neurons neighboring the kth neuron within the receptive field, $x_l(t)$ is the neural activity of the lth neuron at time t, $[x_l(t)]^+ = \max\{x_l(t), 0\}$, and β is a positive scalar constant. The external input I_k of the kth neuron is expressed as

$$I_k = \begin{cases} +E, & k\text{th cell is uncovered} \\ -E, & k\text{th cell is obstacle} \\ 0, & k\text{th cell is already covered} \end{cases} \tag{18}$$

where, E is a positive scalar constant. To maximize the neural activities of uncovered cells and minimize those of cells categorized as obstacles, the value of the external input E should be substantially larger than the weighted sum of incoming signals from lateral connections. For the cells categorized as uncovered (green circles), the neural activity is 1; for the cells marked as an obstacle (brown circles), it is –1; and for the cells covered (pink circles), it is [0, 1).

Initially, all the cells in the loading area are categorized as uncovered, while the others in the grid map are categorized as obstacles. The neural activity of the neurons is initialized accordingly, as shown in Figure 3. The start point of the path planning is set at the end point of the former loading round. For the first loading round, the start point is the lowest cell.

To select the next navigation, the previous GBNN-based complete coverage path planning methods focused primarily on minimizing factors related to robot energy consumption to improve efficiency[25-27]. In these methods, the sequence of coverage to a certain grid cell is determined solely by the location of that cell. However, in the situation presented in this paper, improving the uniformity of loading is the main objective. It is natural to take into account the properties of the area to be covered itself, specifically the height of the grid cell, because loading lower areas results in better loading uniformity.

Since the unloading spout only moves laterally and longitudinally on the horizontal plane and not diagonally, the energy consumed to reach any of the four candidate grid cells is assumed to be equal due to the same travel distance. Only the energy consumed by the change in movement direction and the height of the candidates needs to be considered. The next cell for the movement (defined as s) is selected among the possible neighboring candidates as

$$s = \arg\max_{\forall j \text{within R}}(x_j + \lambda_e e_j + \lambda_h h_j) \tag{19}$$

where, x_j is the neural activity of the jth cell, e_j is the normalized energy efficiency of navigation to the jth cell, and h_j is the normalized height of the jth cell.

Here, $\lambda_e \in [0,1]$ and $\lambda_h \in [0,1]$ control the tradeoff paid for energy usage and the loading uniformity. If they were too high, it would take many steps to recover from a deadlock. On the contrary, the energy- and uniformity-related issues may be overlooked if they are too low. Additionally, if energy or uniformity considerations are given too much weight, the robot may fail to be attracted to uncovered cells when all the neighboring neurons have already been covered. To avoid this undesired behavior, λ_e and λ_h can be dynamically adjusted to adapt to the situation[24]. However, the experimental study revealed that taking energy and uniformity into account may result in a longer complete coverage path with little improvement in energy efficiency or uniformity during loading. In each loading round, the order of coverage has little effect on the loading uniformity since the heights of the cells in the loading area are almost the same. Based on the considerations above, λ_e and λ_h are set to zero to ignore the energy- and height-related issues.

2.3.3 Transfer path planning

In this section, the breadth-first search-based transfer path planning algorithm is proposed for the unloading spout to travel to

another local lowest cell designated by the overflow algorithm. The workspace, start cell, and end cell for path planning can be obtained from the overflow algorithm. An example result of the overflow algorithm is shown in Figure 4a, where the workspace consists of the last loading area (gray cells) and the candidate area (green cells); the start cell and end cell are represented by a red circle and a blue rectangle, respectively.

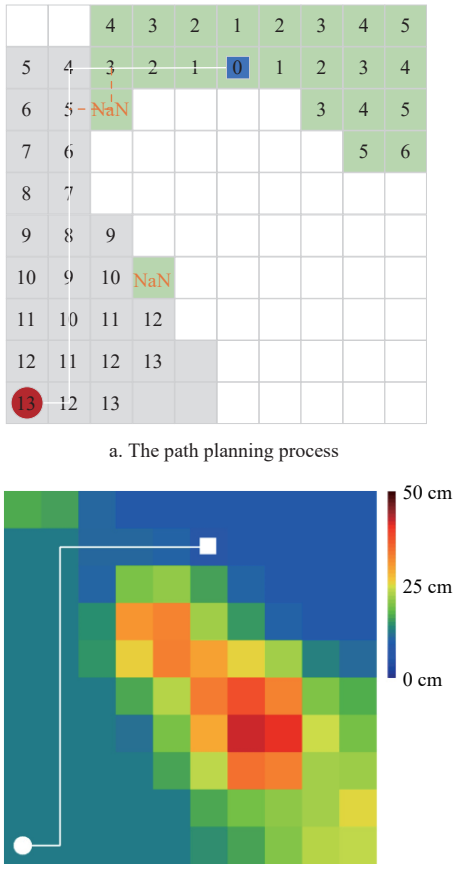

a. The path planning process

b. The loading state

Figure 4 Example results of transfer path planning

Point-to-Point (PTP) path planning is an extensively researched problem that aims to discover a collision-free path with the shortest distance and least time consumption from a defined start point to a designated end point[28]. While the unloading spout moves along the PTP path, the unloading process needs to continue uninterrupted. To improve the uniformity, the path should pass through cells with lower heights. Thus, the path should be optimized for both a shorter distance and lower height. To make a trade-off between the two objectives, a transfer path with the shortest distance that gradually decreases in height is formulated.

First, the key idea of breadth-first search is followed to keep track of an expanding ring called the frontier from the end cell[28]. With the expansion of the frontier, each grid cell is assigned a specific number based on the path distance, starting from 0 at the end cell. As shown in Figure 4a, all the unmarked cells neighboring the marked cell k in four directions receive the label $k+1$, but only if their heights are not lower than that of the cell k. The expansion of the frontier stops as soon as the start cell is found. Subsequently, the path can be obtained by commencing at the start cell and selecting the neighboring cell with the diminishing label. Specifically, for a current cell marked as k ($k>0$), the neighboring cell with the label $k-1$ is selected as the next location. In cases where two or more neighbors share the same label, the one with the lowest height is selected.

Remark 4: The path planning algorithm described above guarantees the identification of a transfer path from the start to the end. This certainty arises from the fact that for any arbitrary cell marked as k, there is at least one neighboring cell marked as $k-1$, and only the end cell is marked as 0 in the entire workspace. The unloading spout can seamlessly follow the resulting path to successfully accomplish the transfer.

Notably, the transfer path obtained from the above process exhibits a decreasing trend in cell height, which follows the idea of water flowing downwards. The visual representation is depicted in Figure 4b, where distinct colors are assigned to different heights. This is ensured by marking only the neighboring grid cells whose height is no lower than that of the current cell. Because the cells with a local minimum height (such as the cells marked as "*NaN*") are not labeled with any number during the whole process, the paths that are not always diminishing (such as the path indicated by the yellow dotted line shown in Figure 4a) are left out. Certainly, the transfer path is also the shortest among all possible diminishing paths.

3 Simulation and discussion

3.1 Numerical simulations

To validate the effectiveness and strong robustness of the proposed loading method against various initial loading states, numerical simulations were conducted in this study. The simulation environment was a 2 m×2 m two-dimensional workspace represented by a discretized grid map of 10×10 cells, where each cell size is defined as 0.2 m×0.2 m. The same initial loading state as the dynamic uniform loading method[17] was adopted for simulation in this study, and the virtual height of each grid cell was initialized to the average height derived from the three-dimensional point cloud data within the range of 0.2 m×0.2 m. In addition, the unloading spout was simplified as a particle, and its shape and size were not considered. When loading grains within a grid cell, the unloading spout was located at the center of the cell. It was assumed that the grains coming from the unloading spout would remain within the cell and not spill out, as the grains were few in quantity.

The simulations were carried out as follows. First, the overflow algorithm was used to assign a loading area for each loading round before a uniform loading state was achieved. The parameters of the overflow algorithm were set as $\Delta h_{\min}=0.02$m and $\Delta h_{\max}=0.04$ m. As described in Algorithm 1, the loading was divided into two different models. In the one case, when the loading area is expanded, a connected region is generated for the improved GBNN algorithm to execute complete coverage path planning. Corresponding to the grid map of 10×10 cells, the neural network in the GBNN comprises 10×10 topologically organized neurons. In each loading round, all the neural activities are reinitialized according to the results of the overflow algorithm. The GBNN algorithm parameters were set as $\alpha=2$, $\beta=0.7$, $E=100$ for the external input, and $R=2$ for the radius of the receptive field. In the other case, when the unloading needs to be transferred to another local lowest cell, the breadth-first search-based planning algorithm is used to guide the transfer. It was assumed that the planned paths for each loading round could be accurately executed by the control system. Therefore, the expected loading results can be adopted in simulations as a replacement for the loading state detection results.

3.1.1 Overflow planning results

The results of the overflow algorithm in several loading rounds are shown in Figure 5. The algorithm started by selecting the grid

cell with the minimum height as the initial position for the unloading spout, as shown by the gray cells in the first round of Figure 5. As the loading proceeded, the loading area expanded until the 5th loading round, where the loading reached the state shown in Figure 5b. Then, the load was transferred to another local lowest cell where the green rectangle was located, as shown in the 6th loading round in Figure 5c. The transfer occurred several times (13th and 20th rounds) during the subsequent loading process. The overflow algorithm assigned a target cell for each transfer round, as shown with the green rectangle. The target cell was set as the loading area in the next loading round. In the other loading round, the loading area gradually expanded before the transfer occurred.

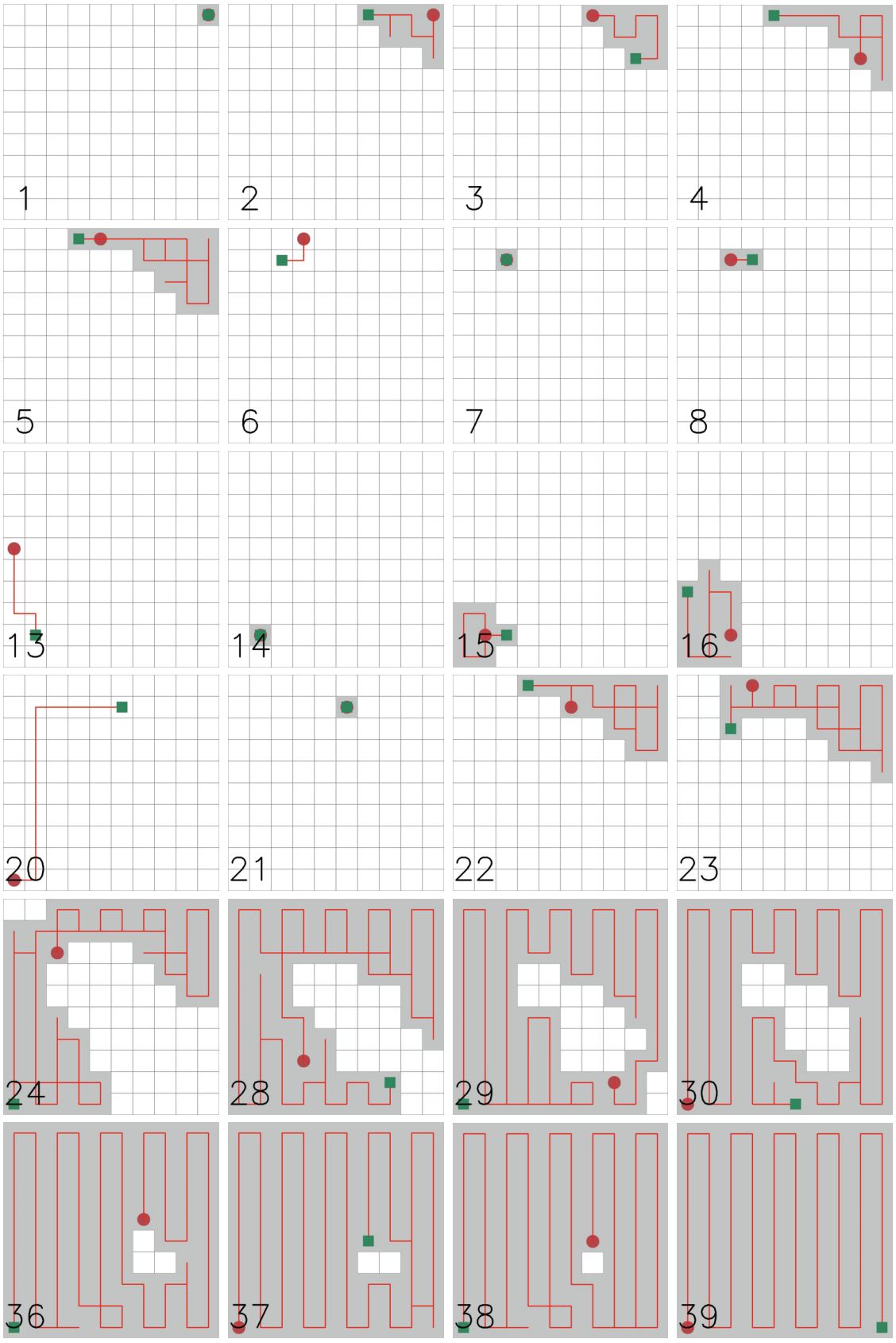

Figure 5 Results of the overflow planning method

In the stage before the 24th loading round, connected areas formed in the upper right corner and the lower left corner successively. In the 24th loading round, these two areas merged to form a larger area, resembling the state depicted in Figure 5d. Up to this moment, the loading area had never involved the higher southeastern area, and loading occurred only in the area with a relatively lower height to improve the loading uniformity. After that, as the grain surface continued rising, the loading area gradually expanded to cover the entire workspace. It should be noted that the highest cell in the initial state (the white cell shown in the 38th round of Figure 5) had never been loaded until the final loading round, during which a uniform loading state was achieved. Therefore, the loading height at the uniform loading state is limited to less than $2\Delta h_{min}$ higher than the highest cell, allowing the uniform loading state to be achieved quickly with as little loading quantity as possible.

The path planning results of the improved GBNN algorithm are illustrated in Figure 5. The start points and the end points are denoted by the red circles and green rectangles, respectively. In the first loading round, the lowest cell was designated as the start point. In subsequent loading rounds, the end point of the previous round was set as the start point. The end point was not preassigned but rather resulted from path planning. Notably, the red path planned in each loading round effectively covered all the gray areas with low repeating coverage. Furthermore, in comparison to the lateral direction, the planned paths hold more longitudinal route segments that align with the travel direction of the vehicle, which is conducive to the implementation of the coordinated control system.

As shown in Figure 4, the workspace of transfer path planning excluded areas with higher cells; thus, the transfer path did not pass through any area with a high loading quantity. The results of the transfer paths can be seen in the 6th, 13th, and 20th rounds of Figure 5. The paths between the starting point and the ending point are the shortest paths that diminish in height, which can minimize the uniformity of the transfer process.

The loading path was continuous because the end point in each round served as the start point in the next round. By moving the unloading spout along the loading path, the loading process can proceed continuously without interruption to make the loading state in the grain tank change from an arbitrary initial state to a uniform state.

3.1.2 Uniform loading results

The overflow algorithm assigned a loading area and target height for each loading round. When the areas obtained at each round were loaded to the corresponding target height, the loading uniformity curve was evaluated by variance, and is shown in Figure 6. Initially, the grain tank exhibited poor loading uniformity, as evidenced by the large variance in height. In the process that followed, the variance in the height decreased slowly because the area to be loaded was small in each loading round. In the middle period, the variance in the height decreased rapidly as the loading area increased. In the later period, since the loading heights in most areas of the grain tank became consistent, the loading height variance decreased slowly as the loading continued. Finally, a uniform loading state was achieved at the 39th loading round when the heights at all the positions became consistent.

Instead of fixing the increment quantity of loading in the grid cells as in the dynamic uniform loading method[17], the overflow algorithm proposed dynamically adjusts the increment quantity of loading to adapt to the different heights of grid cells. Loading from the same initial state, the most uniform loading state evaluated with the variance of height that the overflow algorithm can reach is 0 for the increment quantity in the range of [2 cm, 4 cm], while that which the dynamic uniform loading method can reach is 0.308 cm^2 for the increment quantity of 2 cm, and 1.25 cm^2 for the increment quantity of 4 cm. These results demonstrated that the overflow algorithm can achieve better uniformity in the loading state compared with the dynamic uniform loading method.

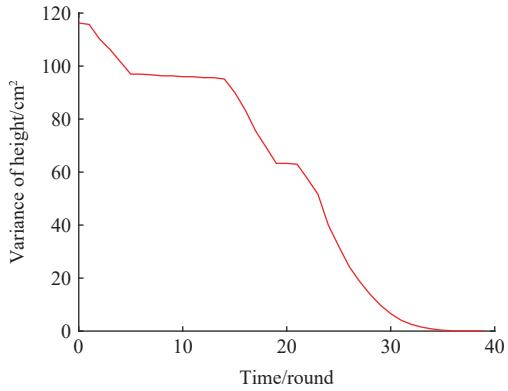

Figure 6 Curve of variance generated from the overflow algorithm

When the unloading spout follows the continuous path shown in Figure 5 to cover all the grid cells specified by the overflow algorithm, sometimes it is inevitable to go through the same grid cell more than once in a single loading round. For a grid cell covered n times in a loading round, the loading quantity each time the unloading spout arrives at that cell is $1/n$ of what it should be loaded. The loading quantity in a special cell can be controlled by the duration which the unloading spout stays on it. Thus, when a loading round ends, all the covered grid cells reach the same target height, as expected. The variance curve during the overflow loading process is shown in Figure 7. In the former period, the loading uniformity of the grain tank was poor, which is shown as a high variance, but it decreased rapidly during the loading process that followed. In the later period, the loading heights in most areas of the grain tank were consistent, and the variance decreased slowly when the loading continued. Finally, the loading state reached a uniform level at step 1851. The loading quantity on the transfer path was ignored because the unloading spout moved quickly on the transfer path with few grains coming out. In fact, these effects can also be eliminated by timely updating the loading state.

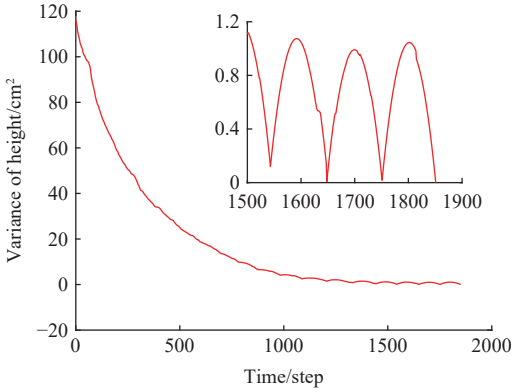

Figure 7 Curve of variance in the overflow loading process

Furthermore, Figure 6 and Figure 7 show that the introduction of the improved GBNN algorithm and breadth-first planning algorithm did not change the trend of uniformity, which had been determined by the overflow algorithm. They were introduced to

obtain the shortest possible path to save energy while meeting the other demands. Other path planning algorithms can also be used to replace them for different trade-offs because the planning framework provided by the overflow algorithm is compatible with all the path planning algorithms.

To verify the effect of the loading increment on the loading process, a comparative simulation experiment was conducted. The loading increment can be expressed as the height increment in cells, which was limited within the range from $\Delta h_{\min}$ to $\Delta h_{\max}$. The loading process for two different sets of parameters is shown in Figure 8. The average height of the grain surface in the grain tank was used to indicate the loading capacity of the grain bin. As the loading proceeded, the variance in the height decreased rapidly, and the loading tended to be uniform, as shown by the solid line in Figure 8. It is worth noting that those with low loading increments will reach the uniform state first. After the loading reached a uniform state, the subsequent loading showed a periodic change, as shown by the dashed line. The uniformity of loading was better during loading with fewer loading increments throughout the loading process with more loading rounds.

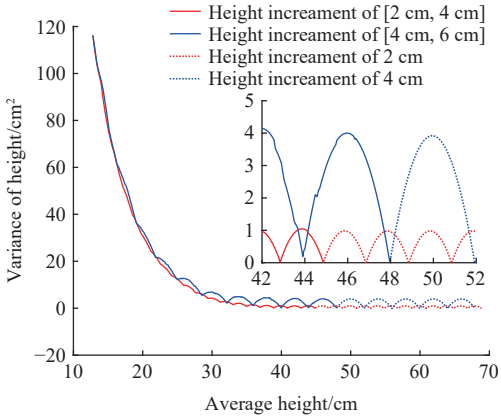

Figure 8 Performance with different increments during loading

3.2 Discussion

3.2.1 Unloading efficiency

The main advantage of the loading path planning method proposed in this paper is its ability to accomplish uniform loading in the grain tank without any interruption over various initial loading states. Although the fixed-point loading method theoretically has the potential to achieve uniform loading by distributing a sufficient number of loading points throughout the grain tank, it often leads to unbalanced loading states during the process. Since the loading is carried out point by point, there is a period of time when some areas become full while others remain empty or have a low quantity of grains. The significant height difference between adjacent areas causes grains to tend to slide from higher areas to lower ones when the transporter encounters bumps in the field. As a result, in practical implementation, the grain tank is unlikely to be fully loaded with the fixed-point loading method. Worse still, it risks grain spillage. Although this issue has been solved in the dynamic uniform loading method by improving the uniformity during loading, the efficiency is limited for discontinuous loading paths. In contrast, the overflow planning method proposed in this paper achieves uniform loading by initially focusing on the lowest area and gradually expanding to encompass the entire grain tank. While improving the uniformity during unloading to reduce the possibility of unexpected changes in the loading state, it ensures the continuity of the loading path. Furthermore, as an online planning method, the overflow planning method can effectively cope with and respond to unforeseen changes in the loading state.

The overflow planning method divides the grain tank into $m \times n$ subregions of the same size and shape. Subregions that are too small pose challenges for separate loading, while subregions that are too large are not conducive to the capacity utilization of the grain tank. The fixed-point loading method can be considered a special case where the grain box is divided into $1 \times n$ subregions, meaning that there is no division in the lateral direction. Consequently, this results in poor loading uniformity with a reduction in loading quantity. To improve the loading quantity, the grain tank should be divided as finely as possible within reasonable limits.

In order to regulate the unloading process, the minimum and maximum height increments, $h_{\min}$ and $h_{\max}$, are introduced to control the gradient of the target height. A smaller gradient results in more loading rounds, thereby improving loading uniformity, while a larger gradient reduces the number of rounds but results in lower uniformity. When the gradient is maximized, the target height is set to the full loading height in the first round, and the loading process degrades into partition loading, where the loading is completed in just one round. The introduction of minimum and maximum height increments allows for a trade-off between loading uniformity and loading rounds to address the specific requirements of the situation.

Once the loading state achieves uniformity, the loading area always maintains the entire grain tank in subsequent rounds. In addition to performing complete coverage path planning in each loading round, another option is to design a fixed path for all subsequent rounds. Among all the complete coverage paths, the spiral Hamiltonian circuit[21] not only demonstrates superior uniformity during loading but also provides enhanced stability and reduces mechanical wear due to its smaller maximum offset from the center of gravity.

3.2.2 Mechanical compatibility

The unloading method proposed in this paper requires the coordination of combine harvesters and transport vehicles. Since the parameters b, c, and l shown in Figure 1 are constant for specific agricultural machinery, they must be properly matched in a cooperative harvesting system as indicated in Equation (7). It is noted from Equation (8) that the parameters b, c, and l directly determine the distance d between vehicles, which will affect the safety of driving. For the design of combine harvester, the value of $l-c$ can be increased appropriately to improve the applicability while still meeting other design requirements.

The applicability of different harvesting setups is the key to the successful application of the method. Some important parameters vary with different harvesting setups, such as the height difference between the unloading port and the grain tank, unloading speed, and the size of unloading port. All these parameters affect the accumulation of grains in the grain tank. Due to the difficulty in accurately modeling their relationship, it is essential to conduct a trial unloading prior to the formal unloading process to account for varying parameters in different harvesting setups. The size of the grid cells into which the grain tank is divided should be set larger than the range of grain accumulation in the empty grain tank within a given unit of time. Through the experimental measurement, not only different harvesting setups, but also different types of grains are taken into consideration.

4 Conclusions

In this paper, a novel unloading method was proposed for continuous co-loading during master-slave navigation harvesting.

Through the strategic motion of the unloading spout, the loading state in the grain tank can transition from an arbitrary initial state to a uniform state, thereby maximizing the capacity utilization of the grain tank and enhancing the harvest efficiency. Additionally, the improved loading uniformity during loading enhances the stability of the transport vehicle, reducing the risk of spillage. The simulation results demonstrated the effectiveness and superiority of the designed unloading method compared with existing methods.

[References]

[1] Alexandratos N, Bruinsma J. World agriculture towards 2030/2050: the 2012 revision. 2012.

[2] Wang K R, Xie R Z, Xue J, Sun L R, Li S K. Comparison and analysis of maize grain commodity quality and mechanical harvest quality between China and the United States. Int J Agric & Biol Eng, 2022; 15(1): 55–61.

[3] Wang Z T, Tang Y R, Jin X Z, Liu Y, Zhang H, Niu H, et al. Comprehensive evaluation of Korla fragrant pears and optimization of plucking time during the harvest period. Int J Agric & Biol Eng, 2022; 15(3): 242–250.

[4] Zhang L, Zhang H D, Chen Y D, Dai S H, Li X M, Imou K, Liu Z H, et al. Real-time monitoring of optimum timing for harvesting fresh tea leaves based on machine vision. Int J Agric & Biol Eng, 2019; 12(1): 6–9.

[5] Kurita H, Iida M, Suguri M, Masuda R. Application of image processing technology for unloading automation of robotic head-feeding combine harvester. Engineering in Agriculture, Environment and Food, 2012; 5(4): 146–151.

[6] Kurita H, Iida M, Suguri M, Masuda R, Cho W. Efficient searching for grain storage container by combine robot. Engineering in Agriculture, Environment and Food, 2014; 7(3): 109–114.

[7] Kurita H, Iida M, Cho W, Suguri M. Rice autonomous harvesting: operation framework. Journal of Field Robotics, 2017; 34(6): 1084–1099.

[8] Delchev N, Trendafilov K. Structural analysis of the operations and time for tank unloading of grain harvesters. International Journal of Science and Research, 2015; 4(3): 1890–1894.

[9] Tihanov G. A study on the hopper unloading duration of the harvesting machine at different technical parameters. Agricultural Science and Technology, 2020; 12(2): 140–143.

[10] Trendafilov K, Delchev N, Kolev B, Tihanov G. Study on the emptying time of grain harvester hoppers. Agricultural Science and Technology, 2017; 9(4): 291–295.

[11] Reinecke M, Grothaus H P, Hembach G, Scheuren S, Hartanto R Dynamic and distributed infield-planning system for harvesting. In: 2013 ASABE Conference, Kansas City, Missouri, July 21-24, 2013. https://elibrary.asabe.org/abstract.asp?aid=43639&t=5

[12] Zhang W, Zhang Z, Luo X, He J, Hu L, Yue B. Position-velocity coupling control method and experiments for longitudinal relative position of harvester and grain truck. Transactions of the CSAE, 2021; 37(9): 1–11. (in Chinese)

[13] Delchev N, Trendafilov K, Tihanov G, Stoyanov Y. Grain combines productivity according to various unloading methods - in the field and at the edge of the field. Agricultural Science and Technology, 2016; 8(3): 221–226.

[14] Liu D, Wang Z, Bai X, Zhao Y. Grain truck loading status detection based on machine vision. In 2019 IEEE 4th International Conference on Image, Vision and Computing (ICIVC), Xiamen, China, 2019. doi: 10.1109/ICIVC47709.2019.8981112

[15] Liu L, Du Y, Li X, Sun T, Zhang W, Li G, Mao E. An automatic forage unloading method based on machine vision and material accumulation model. Computers and Electronics in Agriculture, 2023; 208: 107770.

[16] Liu Z, Dhamankar S, Evans J T, Allen C M, Jiang C, Shaver G M, McDonald B M. Development and experimental validation of a system for agricultural grain unloading-on-the-go. Computers and Electronics in Agriculture, 2022; 198: 107005.

[17] Wang X, Wang Z, Bai X, Ge Z, Zhao Y. Dynamic uniform loading method of grain box of transport vehicle based on three-dimensional point cloud. Transactions of the CSAM, 2022; 53(6): 129–139. (in Chinese)

[18] Ma Z, Chong K, Ma S, Fu W, Yin Y, Yu H, Zhao C. Control strategy of grain truck following operation considering variable loads and control delay. Agriculture, 2022; 12(10): 1545.

[19] Shojaei K. Coordinated saturated output-feedback control of an autonomous tractor-trailer and a combine harvester in crop-harvesting operation. IEEE Transactions on Vehicular Technology, 2022; 71(2): 1224–1236.

[20] Zhang X, Geimer M, Noack P O, Grandl L. Development of an intelligent master-slave system between agricultural vehicles. In IEEE Intelligent Vehicles Symposium (IV), San Diego, CA, 2010. doi: 10.1109/IVS.2010.5548056

[21] Wang X, Wang Z, Bai X, Ge Z, Wang J, Man Z. A loading path planning method for co-loading in automatic harvesting system. In 2023 International Conference on Advanced Mechatronic Systems (ICAMechS), Melbourne, Australia, 2023. doi: 10.1109/ICAMechS59878.2023.10272697

[22] Galceran E, Carreras M. A survey on coverage path planning for robotics. Robotics and Autonomous Systems, 2013; 61(12): 1258–1276.

[23] Liu L, Wang X, Yang X, Liu H, Li J, Wang P. Path planning techniques for mobile robots: Review and prospect. Expert Systems with Applications, 2023; 227: 120254.

[24] Glasius R, Komoda A, Gielen S. A biologically inspired neural net for trajectory formation and obstacle avoidance. Biological Cybernetics, 1996; 74(6): 511–520.

[25] Muthugala M A V J, Samarakoon S M B P, Elara M R. Toward energy-efficient online complete coverage path planning of a ship hull maintenance robot based on glasius bio-inspired neural network. Expert Systems with Applications, 2022; 187: 115940.

[26] Sun B, Zhu D, Tian C, Luo C. Complete coverage autonomous underwater vehicles path planning based on Glasius bio-inspired neural network algorithm for discrete and centralized programming. IEEE Transactions on Cognitive and Developmental Systems, 2019; 11(1): 73–84.

[27] Zhu D, Tian C, Sun B, Luo C. Complete coverage path planning of autonomous underwater vehicle based on GBNN algorithm. Journal of Intelligent & Robotic Systems, 2018; 94(1): 237–249.

[28] Hart P E, Nilsson N J, Raphael B. A formal basis for the heuristic determination of minimum cost paths. IEEE Transactions on Systems Science and Cybernetics, 1968; 4(2): 100–107.